

Combined Effects of Impervious Surface and Vegetation Cover on Air Temperature Variations in a Rapidly Expanding Desert City

Soe W. Myint¹ and Anthony Brazel

School of Geographical Sciences and Urban Planning, Arizona State University, Tempe, Arizona 85287-0104

Gregory Okin

Department of Geography, University of California, Los Angeles, 1255 Bunche Hall, Los Angeles, California 90095

Alexander Buyantuyev

Sino-U.S. Center for Conservation, Energy, and Sustainability Science, Inner Mongolia University, Economics and Management Building, No. 235 Daxue West Road, Hohhot, Inner Mongolia, P.R. China 010021

Abstract: The goal of this study is to improve our understanding of the interactive function of impervious and vegetation covers at different levels of the local and intra-urban spatial scales in relation to air temperatures in an urban environment. A multiple regression model was developed using impervious and vegetation fractions at different scales to predict maximum air temperature for the entire Phoenix metropolitan area in Arizona, USA. This study demonstrates that a small amount of impervious cover in a desert city can still increase maximum air temperature despite abundant vegetation cover.

INTRODUCTION

Vegetation influences urban environmental conditions and energy fluxes by selective reflection and absorption of solar radiation (Gallo et al., 1993) and by the process of evapotranspiration (Owen et al., 1998; Jonsson, 2004). The presence and abundance of vegetation in urban areas has long been recognized as having a strong influence on energy demand and development of the urban heat island (Oke, 1982; Huang et al., 1987; Sailor, 1995; Spronken-Smith and Oke, 1998; Carlson and Arthur, 2000; Bonan, 2002; Weng et al., 2004; Grossman-Clarke et al., 2005; Jenerette et al., 2007). Urban vegetation abundance may also improve air quality and human health (Wagrowski and Hites, 1997) because photosynthesizing plants absorb atmospheric carbon dioxide,

¹Corresponding author; email: Soe.Myint@asu.edu

sunlight, water, and soil nutrients to release oxygen in the process. Urban trees also trap particulate matter and ozone. The loss of trees in our cities not only intensifies the urban heat island effect due to the loss of shade and evaporation, but also reduces the role of the urban forest as principal absorber of carbon dioxide and trapper of other pollutants. Studies in urban climatology have found that urbanization is often associated with warmer climate and more polluted air than their rural environments (Taha, 1996; Streutker, 2002; Arnfield, 2003; Zhou et al., 2004; Brazel et al., 2007). The modification of an urban landscape influences local (micro-), meso-, and even the macro-climate (Lo et al., 1997; Brazel et al., 2000; Quattrochi et al., 2000; Weng, 2001; Lo and Quattrochi, 2003; Voogt and Oke, 2003).

It is well documented that escalating urbanization results in an increased amount of impervious surfaces (Brabec et al., 2002), and it consequently augments the intensity, volume, temperature, and duration of storm water runoff (Booth and Reinelt, 1993; Schueler, 1994; U.S. EPA, 1997). Urban storm water runoff may cause or contribute to water quality degradation by changing natural hydrologic patterns (Hall, 1984; Driver and Troutman, 1989), accelerating natural stream flows (Booth and Jackson, 1997), increasing stream bank erosion (May et al., 1997), destroying aquatic habitat (Booth and Reinelt, 1993; Horner et al., 1997), degrading stream water quality (Schueler, 1994; Booth and Jackson, 1997; May et al., 1997), increasing temperature (Galli, 1990), and elevating pollutant concentrations and loadings (Brabec et al., 2002; Boyer et al., 2002; Roy et al., 2003).

Impervious surfaces, particularly tar roads and parking lots, are generally dark, and hence they can easily warm up the runoff water (Frazer, 2005). On the other hand, impervious areas have higher thermal conductivity than vegetated covers. Urbanization alters the natural ways energy flows through the atmosphere, land, and water systems (Oke, 1982; Lo and Quattrochi, 2003). For example, the temperature trend in Phoenix demonstrated a 5.5°C increase in the minimum temperatures from the late 1940s to present due to rapid expansion of urbanized areas (Brazel et al., 2000). Impervious surfaces are one of the key indicators of urban growth that can be directly quantified (Arnold and Gibbons, 1996; Brabec et al., 2002). With the advent of urban sprawl, impervious surfaces have become a key parameter to be considered in urban growth and sprawl management because of their impacts on habitat health (Arnold and Gibbons, 1996). Therefore, identification of spatial patterns, percent distribution, and growth of impervious surfaces in an urban-suburban environment is an important step toward effective decision making for urban planning and overall watershed management.

The goal of this study is to improve our understanding of the role of percent distribution of impervious and vegetation covers at different spatial scales in controlling patterns of air temperature at different spatial scales in an urban environment. The study area selected is the Phoenix metropolitan area in Arizona, located in the Sonoran Desert. We develop a multiple regression model using impervious and vegetation fractions at different spatial scales to predict maximum air temperature for the entire Phoenix metropolitan area. We combine remote sensing techniques with climate data to address the role of interactive effects of impervious and vegetation covers on air temperatures in this rapidly urbanizing landscape.

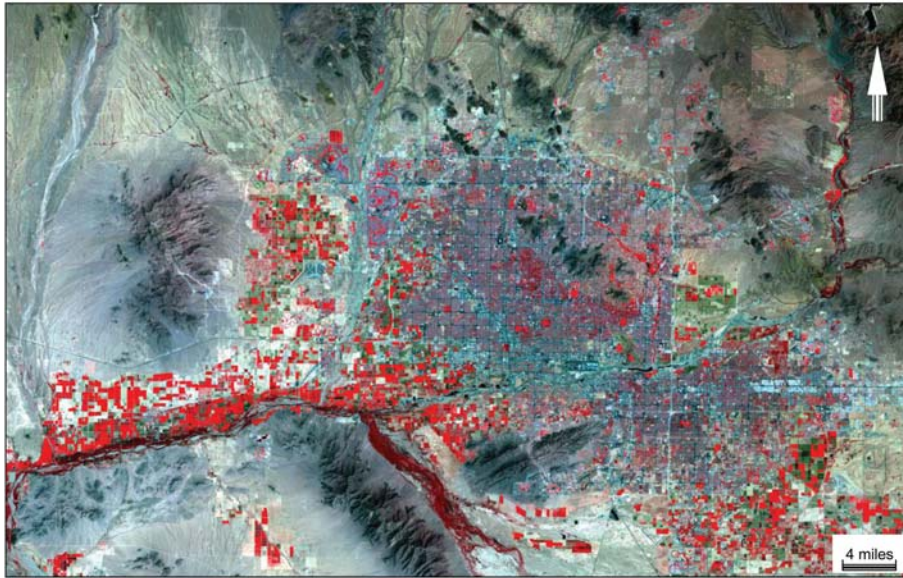


Fig. 1. A false-color composite of Landsat ETM+ 30-meter resolution data over the Phoenix metropolitan area by displaying channel 4 (0.750–0.900 μm), channel 3 (0.630–0.690 μm), and channel 2 (0.525–0.605 μm) in red, green, and blue, respectively.

DATA AND STUDY AREA

A Landsat ETM+ image (L1G product of path 37 and row 37) at 30 m spatial resolution with six channels ranging from blue to the shortwave infrared portion of the spectrum was used to quantify varying amounts and distribution of impervious (surface), vegetation, soil, and shade in urban and suburban areas. The image data was acquired over the Phoenix metropolitan area under cloud-free conditions on April 19, 2000. The original image was subset to extract the Phoenix metropolitan area (upper left longitude W 112°47'10.96'' and latitude N 33°49'59.62'', lower right longitude W 111°34'18.56'' and latitude N 33°12'09.81'').

The Phoenix metropolitan area selected for the study is shown in Figure 1 by displaying Landsat ETM+ channel 4 (0.750–0.900 μm), channel 3 (0.630–0.690 μm), and channel 2 (0.525–0.605 μm) in red, green, and blue, respectively. The study area covers major urban/suburban land use and land cover classes: high-density residential, low-density residential, commercial, wild grass, woodlands, manmade grass, riparian vegetation, agriculture, cement roads, tar roads, cement/tar parking, river, lakes, sandbars, and exposed soil. We used a Quickbird 2.4-meter spatial resolution multispectral image with four channels—blue (0.45–0.52 μm), green (0.52–0.60 μm), red (0.63–0.69 μm), and near infrared (0.76–0.90 μm)—and the accompanying 60 cm panchromatic image (0.45–0.90 μm) acquired over downtown Phoenix on July 11, 2005, to assess the accuracy of percentages of impervious surface, soil, vegetation, and shaded areas at sub-pixel resolution. The selected multispectral Quickbird image

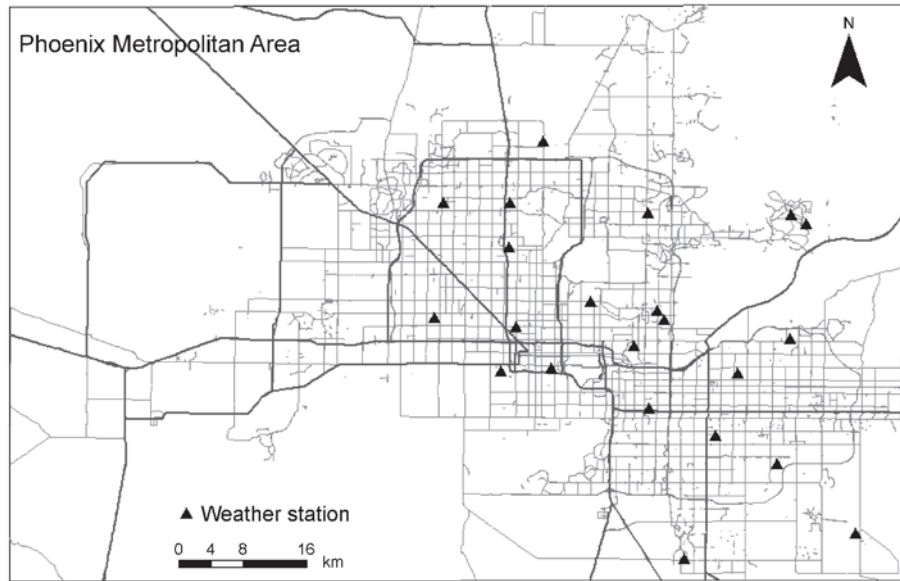


Fig. 2. Selected weather stations located in the Phoenix metropolitan area.

was pan-sharpened to convert from 2.4 meters to 1 meter resolution image data. Both Quickbird and Landsat ETM+ data were orthorectified.

We obtained climate data (daily maximum, minimum, and mean temperature) that were compiled by the Central Arizona–Phoenix Long-Term Ecological Research (CAP-LTER) project from major national, state, and local meteorological networks with weather stations distributed evenly over the Phoenix metropolitan area. Only air temperature data were used for the study. In particular, we used daily air temperature measured within the urban canopy layer (ca. 2 m height) by four networks: (1) Phoenix Realtime Instrumentation for Surface Meteorological Studies (PRISMS; Pon et al., 1998); (2) Arizona Meteorological Network (AZMET; see <http://ag.arizona.edu/azmet>); (3) Maricopa County Flood Control District (MCFCD; see <http://fcd.maricopa.gov>); and (4) co-op stations obtained from the National Climatic Data Center of the National Oceanic and Atmospheric Administration (NCDC, NOAA; data available from www.ncdc.noaa.gov and summarized monthly at www.wrcc.dri.edu). Locations of weather stations used in our study are presented in Figure 2. We extracted air temperatures recorded at the above stations on April 19, 2000.

METHODOLOGY

Spatial Distribution of Impervious, Soil, and Vegetation

Linear spectral mixture analysis (SMA), which is capable of quantifying subpixel endmember fractions, is probably the most commonly used technique of all subpixel analysis techniques. An endmember is the spectrum of a pure land cover (e.g., vegetation, soil, water) and hence SMA endmember fractions are typically interpreted as ground component fractions.

SMA is defined as:

$$X_i = \sum_{k=1}^n f_k X_{ik} + e_i, \quad (1)$$

where X_i is the spectral reflectance of band i of a pixel, n is the number of endmembers, f_k is the fraction of an endmember k within a pixel, X_{ik} is the known spectral reflectance of endmember k within the pixel in band i , and e_i is the error term for band i . The root mean square (RMS) error is given by:

$$RMS = \left[\frac{\sum_{j=1}^m (e_{ij})^2}{m} \right]^{0.5}, \quad (2)$$

where e_i are the error terms for each of the m spectral bands considered. The application of SMA to remote sensing imagery typically also adds the additional constraints that $\sum_{k=1}^n f_k = 1$ and $0 \leq f_k \leq 1$. Because f_k requires solving a system of m or $m +$

1 (when the sum of fractions is forced to be 1), the number of endmembers cannot exceed the number of bands, m . This is a major limitation in modeling urban land covers with the SMA technique when dealing with commonly used remotely sensed data such as IKONOS, SPOT, IRS, ASTER, and Landsat TM, because they normally contain fewer than or equal to seven bands. On the other hand, urban land covers are composed of many spectrally different materials in a small area (e.g., plastic, metal, rubber, glass, tar, cement, wood, shingle, sand, gravel, brick, stone, soil, grass, trees, shrubs, water) (Myint and Lam, 2005). Another limitation is that a standard SMA approach employs an invariable set of endmembers to quantify fractions in all pixels. It should be noted that the number and type of land cover components are highly variable. The endmembers used in SMA are the same for each pixel, regardless of whether the ground components represented by the endmembers are present in the pixel. Hence, we employed multiple endmember spectral mixture analysis (MESMA), an extension of the SMA approach that allows the number and type of endmembers to vary for each pixel within an image.

The subpixel approach that we employed in this study is based on a model proposed by Ridd (1995) that land cover in an urban environment is a linear combination of three land cover types (i.e., impervious, soil, vegetation). Our MESMA approach starts with the selection of a set of endmembers that represent pure spectra of the land covers in the scene. The algorithm selects the model with the lowest RMS error for each pixel, with the condition that the RMS error of the best-fit model may not exceed some user-defined threshold. For the best-fit model for each pixel, the fraction values for each endmember and the identity of those endmembers are recorded.

We selected endmembers manually by visualizing the pixel purity index (PPI) results of spectrally pure pixels identified using the PPI in an N -dimensional visualizer with ENVI software package. We geographically linked the PPI image to the original image and high-resolution Quickbird image to identify the image endmembers.

Selected endmembers were grouped into three classes: impervious surfaces (e.g., tar roads, cement roads, different types of rooftops, swimming pools, parking lots); vegetation (e.g., grass, shrubs, desert scrub, trees); and soil (e.g., exposed soil, sand bars, inactive agriculture, recently plowed fields, cleared ground for construction). We employed 28 endmembers and 544 endmember models to identify fractions of soil, impervious surface, vegetation, and shade in the Phoenix metropolitan area.

The detailed methodology employed in the study and validation of output fraction images were presented in Myint and Okin (2008). The mean RMS error for the selected land use and land cover classes range from 0.003 to 0.018. The Pearson correlation between fraction outputs from MESMA and reference data from Quickbird 60 cm resolution data were 0.8041 for soil, 0.8166 for impervious, and 0.8032 for vegetation. We acknowledge that the differences in the dates of the acquisition of Landsat ETM+ and Quickbird could also be considered a possible limitation in effectively assessing the accuracy. Our accuracy analysis minimized these problems by reselecting only those reference points that did not change between 2000 and 2005. We first looked at apparent changes in land use, then land cover, based on the two images and a later 2005 Landsat image. This analysis was further reinforced by ground-based verification.

Results from the study demonstrated that the selected models were reliable, and the MESMA algorithm quantified the selected endmembers (i.e., impervious, vegetation, soil) accurately (Myint and Okin, 2008). Figures 3 and 4 show percentages of impervious and vegetation distribution of the Phoenix metropolitan area, respectively. We generated mean percentage distribution of impervious and vegetation using different window sizes ranging from 3×3 to 33×33 pixels. This was done to obtain percentage distribution of impervious surface and vegetation for varying areal extents.

Regression Analysis

We extracted percent distribution of impervious and vegetation from the original image ($30 \text{ m} \times 30 \text{ m}$) and the above output images with mean fraction values generated with the use of different window sizes. Extracted fraction values of impervious and vegetation were integrated with weather data. A linear regression analysis was performed to determine the correlation between air temperature (maximum and minimum) and percent distribution of impervious and vegetation at different spatial scales (i.e., 30 m to 990 m). Parameters from models with the highest correlations (e.g., impervious percent distribution in $30 \text{ m} \times 30 \text{ m}$ neighborhood, vegetation percent distribution in $270 \text{ m} \times 270 \text{ m}$ neighborhood) were used to develop a multiple regression model to predict air temperature for the entire Phoenix metropolitan area. This was done to evaluate interaction effects of impervious and vegetation covers that influence the urban heat island in this rapidly growing city. In addition to standard statistical parameters (e.g., correlation, coefficient of determination, standard error, t statistics, etc.), we computed root mean square error (RMS) and bias to demonstrate the strength of the model. This was also supported by a residual plot of the model.

RESULTS AND DISCUSSION

Maximum Air Temperature vs. Impervious

As mentioned earlier, we performed a regression analysis to compute the correlation between fractions of impervious surface and maximum air temperature recorded



Fig. 3. Impervious fraction layer of the Phoenix metropolitan area. White = 100%; black = 0%.



Fig. 4. Vegetation fraction layer of the Phoenix metropolitan area. White = 100%; black = 0%.

on April 19, 2000. The wind during the entire day was less than 5 mph and thus strong advective effects long distances from weather sites are likely minimized. It was found that percent impervious surface covers within different areal extents were positively

Table 1. Correlation Coefficients between Air Temperature and Percent Distribution of Impervious and Vegetation with the Use of Different Window Sizes

Windows	Correlation coefficients			
	Max. Temp. vs. Imp.	Max. Temp. vs. Veg.	Min. Temp. vs. Imp.	Min. Temp. vs. Veg.
30 m × 30 m	0.430	0.016	0.684	0.184
90 m × 90 m	0.371	0.211	0.533	0.271
150 m × 150 m	0.387	0.276	0.586	0.185
210 m × 210 m	0.386	0.328	0.593	0.149
270 m × 270 m	0.298	0.324	0.524	0.147
330 m × 330 m	0.263	0.294	0.517	0.174
390 m × 390 m	0.225	0.294	0.543	0.167
450 m × 450 m	0.237	0.252	0.552	0.171
510 m × 510 m	0.191	0.219	0.533	0.187
570 m × 570 m	0.204	0.196	0.535	0.210
630 m × 630 m	0.202	0.176	0.546	0.222
690 m × 690 m	0.208	0.177	0.550	0.219
750 m × 750 m	0.177	0.165	0.552	0.206
810 m × 810 m	0.186	0.167	0.547	0.211
870 m × 870 m	0.187	0.151	0.551	0.214
930 m × 930 m	0.185	0.126	0.558	0.215
950 m × 950 m	0.197	0.115	0.534	0.212

correlated with maximum air temperature. The computed correlations between maximum air temperature and percent impervious per unit area ranging from 30 m × 30 m to 990 m × 990 m were 0.430, 0.371, 0.387, 0.386, 0.298, 0.263, 0.225, 0.237, 0.191, 0.204, 0.202, 0.208, 0.177, 0.186, 0.187, 0.185, and 0.197 (Table 1). The correlation coefficient drops after about 210 m × 210 m and the curve flattened after about 390 m × 390 m (Fig. 5). This implies that impervious percent distribution within a neighborhood ranging from 30 m × 30 m (original pixel resolution) to 210 m × 210 m affected maximum air temperature most significantly. In other words, high percent distribution of impervious surface within 210 m × 210 m substantially increases maximum air temperature and vice versa. The result also indicates that high or low percent impervious covers in a window size larger than 270 m do not have a strong impact on maximum air temperature. This suggests that under the very calm conditions experienced, the source area impacting temperature was quite local. Correlation was the highest at the original pixel size (30 m), implying that the impervious surface fraction in the smallest area (30 m × 30 m) has the strongest impact on maximum air temperature.

Maximum Air Temperature vs. Vegetation

Percent distribution of vegetation cover computed within areas of different sizes was negatively correlated with maximum air temperature. Correlations computed for

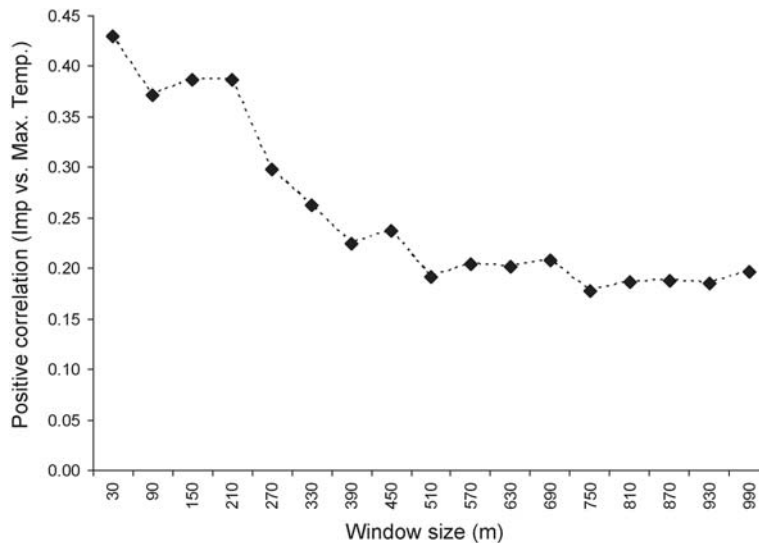


Fig. 5. Correlation coefficients between maximum air temperature and impervious fraction values generated with the use of different window sizes. Abbreviations: Imp. = impervious; Max. = maximum; Temp. = temperature.

maximum air temperature and vegetation cover percent per unit area ranging from 30 m × 30 m to 990 m × 990 m were 0.016, 0.211, 0.276, 0.328, 0.324, 0.294, 0.294, 0.252, 0.219, 0.196, 0.176, 0.177, 0.165, 0.167, 0.151, 0.126, and 0.115 (Fig. 6; Table 1). Percent cover of vegetation at the finest scale (30 m) does not explain maximum air temperature. In other words, a high percentage of vegetation cover in an area less than 30 m × 30 m does not lower the maximum temperature and vice versa. As we increase the window size, correlations between the two variables increase exponentially until it reaches the peak at about the 210 m × 210 m and 270 m × 270 m windows. This pattern suggests that higher abundance of vegetation at these reasonably large scales (i.e., 210 m × 210 m and 270 m × 270 m) can decrease maximum temperature in Phoenix. However, these window sizes are not necessarily going to be the optimal scale if cities in other environmental settings are analyzed. The curve goes down after the 390 m × 390 m window size, and stays almost at the same level after 570 m × 570 m. This implies that percent distribution of vegetation cover in windows larger than 390 m does not have a continually increasing strong influence on maximum air temperature, and hence vegetation abundance at these scales is not really effective in lowering the maximum air temperature at the local site. Upmanis et al. (1998) demonstrated that the magnitude of the temperature difference between a park and its urban surroundings increases with increasing park size. They also found that temperature difference is related to the distance from the park edge. Although their study focused only on parks and did not examine areas away from park edges in a consistent manner, our results generally agree with their findings. However, our results reflect the relation between vegetation and air temperature in the environment where the average summer high temperature exceeds 100°F (38°C), making Phoenix the hottest of any populated area in the United States (<http://www.wordtravels.com/Cities/Arizona/Phoenix/Climate>).

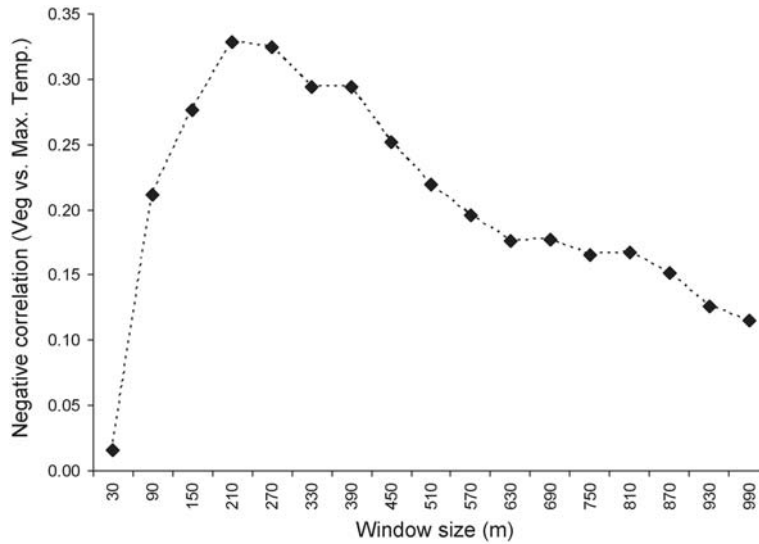


Fig. 6. Correlation coefficients between maximum air temperature and vegetation fraction values generated with the use of different window sizes. Abbreviations: Veg. = vegetation; Max. = maximum; Temp. = temperature.

Interestingly, the effect of vegetation on temperature is not dependent on vegetation type. Although vegetation in our study is considered as one land cover class, the relationship between this clumped vegetation cover and air temperature is robust.

Minimum Air Temperature vs. Impervious

There is a strong positive relation between percent distribution of impervious areas and minimum air temperature. The computed correlations between minimum air temperature and percent of impervious per unit area ranging from 30 m × 30 m to 990 m × 990 m were 0.68, 0.53, 0.59, 0.59, 0.52, 0.51, 0.54, 0.55, 0.53, 0.54, 0.55, 0.55, 0.55, 0.55, 0.56, and 0.53 (Fig. 7; Table 1). These correlations were more scale independent and significantly higher than relationships between maximum air temperature and percent impervious surface. This suggests that a higher percentage of impervious surfaces increases minimum air temperature regardless of neighborhood size or local window size. This is realized due to the role of daytime absorption and heat storage that is expressed in heat retention at night.

Minimum Air Temperature vs. Vegetation

It is important to note that there turned out to be a weak but significant positive relationship between percent vegetation cover and minimum air temperature. Correlations between minimum air temperature and percent vegetation per unit area ranging from 30 m × 30 m to 990 m × 990 m were 0.18, 0.27, 0.19, 0.15, 0.15, 0.17, 0.17, 0.17, 0.19, 0.21, 0.22, 0.22, 0.21, 0.21, 0.21, 0.22, and 0.21 (Table 1). These correlation values were low compared to those between minimum temperature and

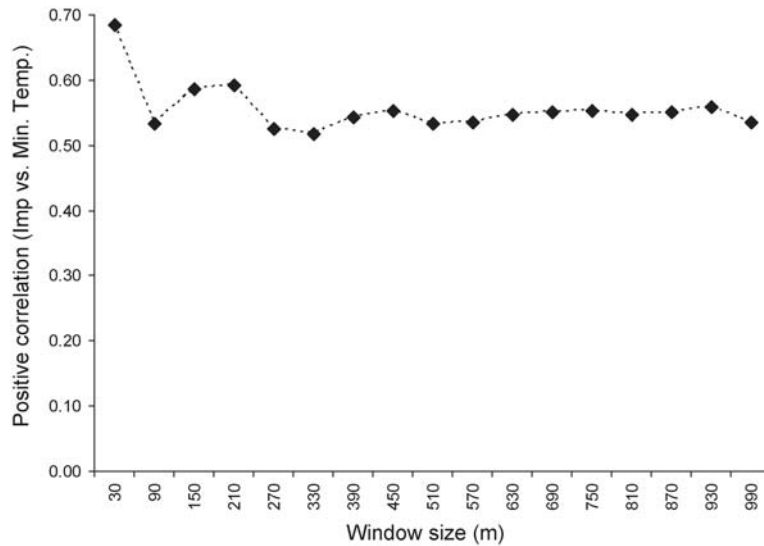


Fig. 7. Correlation coefficients between minimum air temperature and impervious fraction values generated with the use of different window sizes. Abbreviations: Imp. = impervious; Min. = minimum; Temp. = temperature.

percent impervious surface. The positive relation to vegetation was somewhat unexpected and needs to be explored further. However, there are findings elsewhere that are similar, where under and near tree canopies at night there is little mixing to dissipate heat and heat is retained more than open areas due to decreased sky view factors. Solar radiation that penetrates a low-density canopy during the day heats local surfaces that cannot radiate effectively to the night sky (e.g., Myrup et al., 1991; Heisler et al., 1995). The highest correlation was achieved when a 90 m × 90 m local window was considered. Correlations for all other window sizes did not differ from one another (Fig. 8). We can speculate that somewhat higher vegetation cover influences heat retention at night even though it may have reduced maximum temperatures during the day. This is because minimum air temperature is reached in early morning and by then open manmade features and especially soil have cooled more than the ground areas near and under trees.

Multiple Regression Model

Because percent impervious surface at the original spatial resolution and percent vegetation cover within a 7 × 7 pixel local window (210 m × 210 m) exhibited the highest correlations, we used them as independent variables to predict maximum air temperature for the entire metropolitan area of Phoenix. We believe that the multiple regression model developed using the two variables was effective (Table 2). This is also confirmed by a comparison of the original maximum air temperature with the predicted one (Fig. 9), as well as the residual plot of the model (Fig. 10). RMS error (Table 2) stems largely from the outlier at weather station number 12 (Figs. 9 and 10). Removing it would reduce the RMS error, bias, residual, standard error, and improve

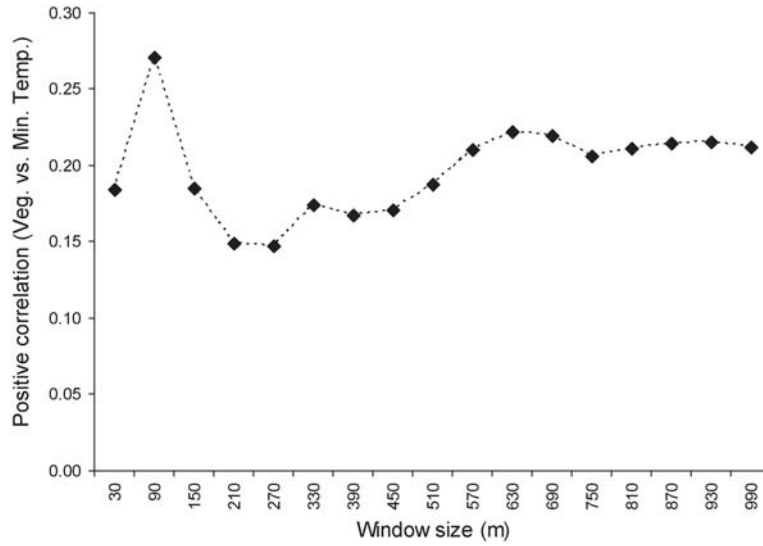


Fig. 8. Correlation coefficients between minimum air temperature and vegetation fraction values generated with the use of different window sizes. Abbreviations: Veg. = vegetation; Min. = minimum; Temp. = temperature.

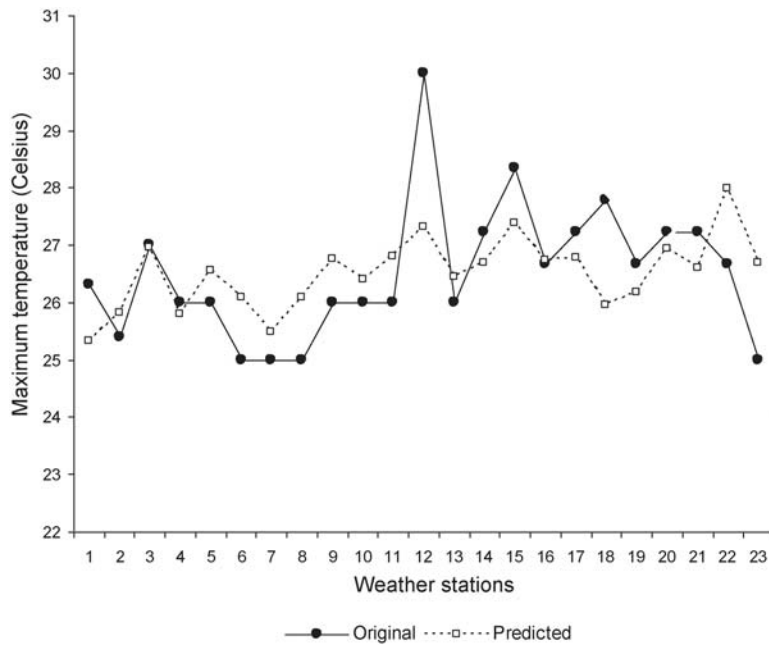


Fig. 9. Model estimates of maximum air temperature compared with the original field measurements of maximum air temperature collected at the weather stations.

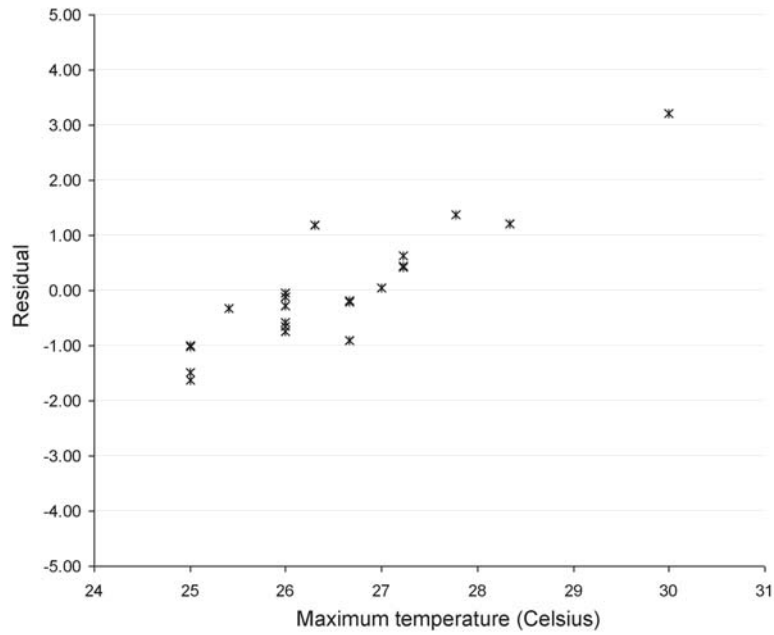


Fig. 10. Residual plot of the regression model.

Table 2. Regression Statistics

Statistic	Value
Multiple R	0.5223
R^2	0.2728
Adjusted R^2	0.2001
RMS error	0.9966
Observations	23.0000
Bias	-0.0001

multiple R and the coefficient of determination significantly. We, however, prefer to keep it because no evidence exists that this is a measurement or instrumentation error. The regression model is highly significant and strong. It helps us explore the interaction of vegetation cover and manmade structures and their combined effects on urban heating in the Phoenix metropolitan area.

The maximum air temperature map of the area (Fig. 11) predicted by this regression model effectively communicates the spatial structure of the urban heat island of Phoenix. The multiple regression model developed in the study is defined as

$$T_c = 26.43 + 1.87(i_{30}) = 2.54(v_{270}), \quad (3)$$

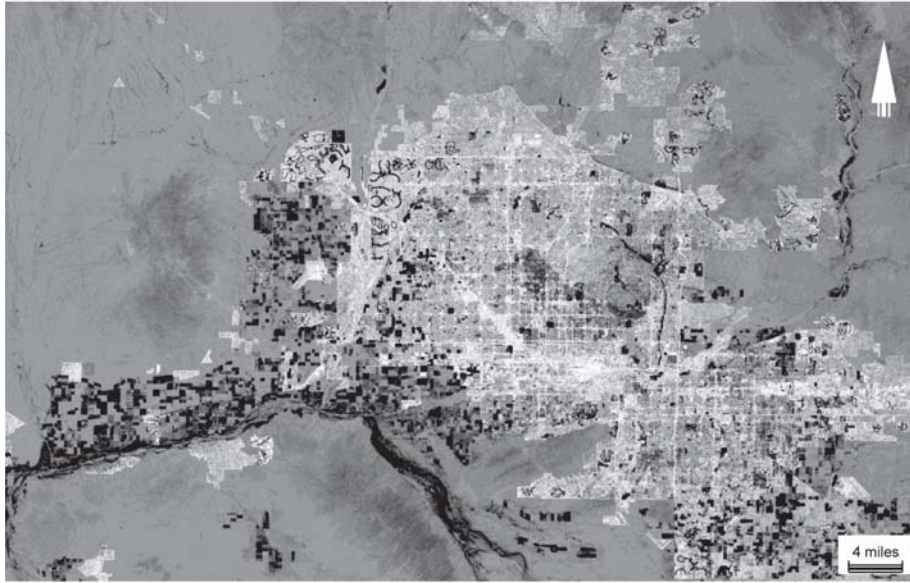


Fig. 11. Model-estimated maximum air temperature of the Phoenix metropolitan area.

where T_c is the maximum air temperature (Celsius); i_{30} is the percent impervious surface area in a $30 \text{ m} \times 30 \text{ m}$ neighborhood; and v_{270} is the percent vegetation cover in a $270 \text{ m} \times 270 \text{ m}$ neighborhood.

The coefficients, standard error, t statistic, and p -values are presented in Table 3. We tested our multiple regression model for multicollinearity, a common limitation of multiple regression models in not being able to distinguish individual effects of two or more independent variables on an outcome variable (Belsley et al., 1980). The problem generally arises when two or more variables are more correlated with each other than they are with the dependent variable. We assessed multicollinearity by examining two collinearity indicators—tolerance and the variance inflation factor (VIF). Tolerance is computed as $1 - R^2$. A small tolerance value suggests that the dependent variable is strongly influenced by a linear combination of independent variables included in the model. The individual effect of each independent variable in this case is difficult to assess. VIF is computed as $1/\text{tolerance}$, and is always greater than or equal to 1. It quantifies the degree to which multicollinearity increases the instability of regression coefficients (Freund and Littell, 2000). There is no formal criterion for determining tolerance or VIF values that can be used to make a decision on whether multicollinearity exists in a regression model. It is generally considered that a tolerance value less than 0.1 or a VIF value greater than 10 imply significant multicollinearity. However, if the relationship between variables is weak, a VIF value between 2.5 and 10 may be regarded as a concern. Klein (1962) suggested an alternative criterion by comparing the coefficient of determination for regression of independent variables (R_k^2) and the original model's R^2 . Significant multicollinearity is detected when $R_k^2 > R^2$. We did not find a multicollinearity problem in our model (Table 4). The tolerance and VIF values for the selected independent variables (i.e., percent impervious surface at the original

Table 3. Model Parameters

	Coefficients	Standard error	<i>t</i> -statistic	<i>p</i> -value
Intercept	26.43	0.59	44.66	0.00
Impervious (30 m)	1.87	0.88	2.11	0.05
Vegetation (270 m)	-2.54	1.62	-1.57	0.13

Table 4. Collinearity Statistics

		Imp-30 m	Max. Temp.	Max. Temp.
Veg-210 m ^a	<i>R</i>	-0.0759		
	Sig. (2-tailed)	0.7307		
	<i>N</i>	23		
Imp-30 m ^b	Pearson <i>R</i>		0.4304	
	Sig. (2-tailed)		0.0403	
	<i>N</i>		23	
Veg-210 m ^a	Pearson <i>R</i>			-0.3280
	Sig. (2-tailed)			0.1265
	<i>N</i>			23

^aTolerance = 0.9942; VIF = 1.0058.

^bTolerance = 0.9942; VIF = 1.0058.

spatial resolution, percent vegetation cover within a 210 × 210 local window) were 0.9942 and 1.0058, respectively (Table 4). The R^2 of our model (0.273) was higher than R_k^2 (0.0058), which supports that our regression analysis is not prone to the problem of multicollinearity.

The model demonstrates the interactive nature of vegetation and manmade features and their relative contribution to altering maximum air temperature in the rapidly growing desert city. Impervious surface areas directly contribute to urban heating and air temperature increases whereas vegetation cover effectively lowers the maximum air temperature. The model implies that in Phoenix an increase in impervious surface area by one unit (100% cover or fractional value of 1) will elevate maximum air temperature by 1.87°, whereas an increase in vegetation cover by 1 unit (100% coverage or fractional value of 1) will lower maximum air temperature by 2.54°. The model seems to imply that vegetation cover can lower air temperature more effectively compared to the ability of impervious areas to increase maximum air temperature. However, it should be noted that percent impervious surface was obtained at 30 m pixel size (original spatial resolution), whereas vegetation fraction values were computed in 270 m × 270 m (9 × 9 window size). This suggests that to lower air temperature we would need to have large patches of dense vegetation, while only a small patch in the same

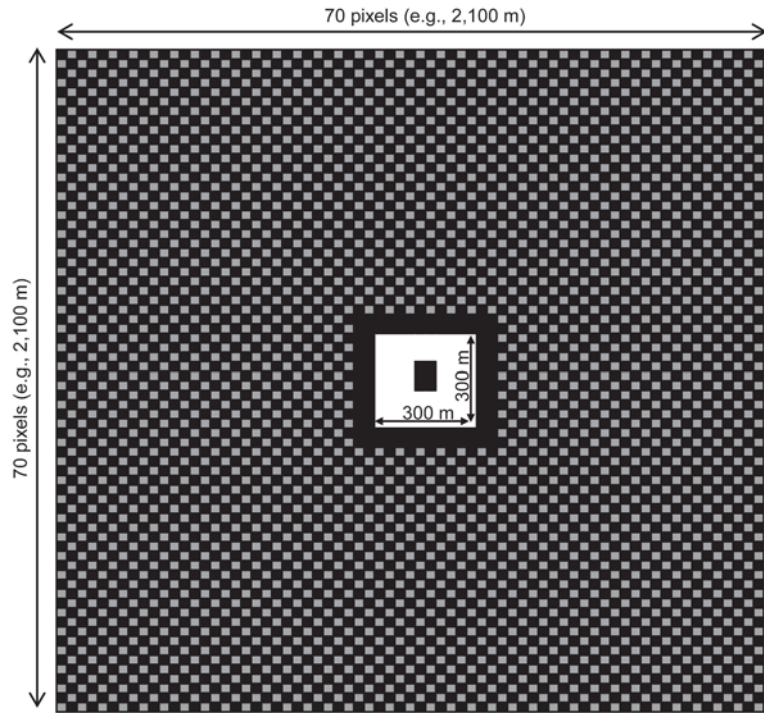


Fig. 12. A hypothetical image of an urban area that can increase maximum air temperature about 0.5° C. White = impervious; black = vegetation; grey = other land covers (e.g., soil, water).

neighborhood dominated by impervious area is capable of raising temperature significantly. According to the model, an area of 270 m × 270 m covered by 50% vegetation will increase the maximum air temperature by approximately 0.5°C if the same area contains only about 1.92% of impervious surface. A hypothetical image is, therefore, created to illustrate this situation (Fig. 12). In this figure, vegetation, impervious surface, and other land covers (e.g., exposed soil, water) are shown in black, white, and grey, respectively. It demonstrates that a small impervious area (94 cells out of 4900 cells ~ 1.92% of impervious coverage) can still increase maximum air temperature by about 0.5°C even though this impervious surface is surrounded by a large area occupied by vegetation (2446 cells/4900 cells ~ 50% coverage). Note that there is no impervious surface in any other area except a small white area in the middle of the square area. In the real world situation, a small fraction of impervious surface and high percentage of vegetative cover could rarely be found in a desert city like Phoenix, especially in commercial, industrial, or high-density residential areas.

CONCLUSION

We examined the role of percent cover of impervious surface and vegetation at a range of spatial “grain sizes.” We developed a multiple regression model using fractions of impervious and vegetation cover at different spatial scales to predict maximum

air temperature for the study area. It demonstrated the combined effects of impervious surfaces and vegetation cover and their influence on the urban heat island effect in a rapidly urbanizing desert city.

Results from this study suggest that we need a sufficiently dense vegetation cover that occupies a reasonably large area (i.e., 210 m × 210 m and 270 m × 270 m) to lower the maximum temperature in Phoenix. Neither dense nor sparse vegetation cover within a given area of 390 × 390 m or larger have an increasing, further effect on maximum air temperature. This implies that vegetated patches within a 390 m range from a particular location do not affect maximum air temperature at that location. This may not be the case for cities in tropical, temperate, or polar climates. Vegetation distribution in a much smaller area does not appear to have an influence on maximum air temperature recorded at a height of 1.5 m. The percent distribution of impervious surface has an immediate effect on maximum air temperature at the finest resolution (30 m). Higher percentages of urban vegetation may lead to slight increases in minimum air temperature. It should be noted that a small amount of impervious cover can still increase maximum air temperature even though there is a large amount of vegetation cover in a rapidly growing desert city. Our findings have potential applications in mitigating urban heat island effects in the Phoenix metropolitan area.

ACKNOWLEDGMENTS

This research was funded, in part, by the National Science Foundation under Grant No. DEB-0423704, Central Arizona–Phoenix Long-Term Ecological Research (CAP LTER). The authors wish to thank the anonymous reviewers for their constructive comments and suggestions.

REFERENCES

- Arnfield, A. J., 2003, "Two Decades of Urban Climate Research: A Review of Turbulence, Exchanges of Energy and Water, and the Urban Heat Island," *International Journal of Climatology*, 23:1–26.
- Arnold, C. L. and C. J. Gibbons, 1996, "Impervious Surface Coverage: The Emergence of a Key Environmental Indicator," *Journal of the American Planning Association*, 62(2):243–258.
- Belsley, D. A., Kuh, E., and R. E. Welsch, 1980, *Regression Diagnostics: Identifying Influential Data and Sources of Collinearity*, New York, NY: John Wiley and Sons.
- Bonan, G. B., 2002, *Ecological Climatology: Concepts and Applications*, Cambridge, UK: Cambridge University Press.
- Booth, D. B. and R. C. Jackson, 1997, "Urbanization of Aquatic Systems: Degradation Thresholds, Stormwater Detection, and the Limits of Mitigation," *Journal of the American Water Resources Association*, 33(5):1077–1090.
- Booth, D. B. and L. E. Reinelt, 1993, "Consequences of Urbanization on Aquatic Systems—Measured Effects, Degradation Thresholds, and Corrective Strategies," in *Watersheds '93*, conference sponsored by the U.S. Environmental Protection Agency, Alexandria, Virginia, March 21–24, 545–550.

- Boyer, E. W., Goodale, C. L., Jaworski, N. A. and R. W. Howarth, 2002, "Anthropogenic Nitrogen Sources and Relationships to Riverine Nitrogen Export in the Northeastern USA," *Biogeochemistry*, 57(1):137–169.
- Brabec, E., Schulte, S., and P. L. Richards, 2002, "Impervious Surfaces and Water Quality: A Review of Current Literature and Its Implications for Watershed Planning," *Journal of Planning Literature*, 16(4):499–514.
- Brazel, A. J., Selover, N., Vose, R., and G. Heisler, 2000, "The Tale of Two Climates: Baltimore and Phoenix LTER sites," *Climate Research*, 15:123–135.
- Brazel, A., Gober, P., Lee, S. J., Grossman-Clarke, S., Zehnder, J., Hedquist, B., and E. Comparri, 2007, "Determinants of Changes in the Regional Urban Heat Island in Metropolitan Phoenix (Arizona, USA) between 1990 and 2004," *Climate Research*, 33:171–182.
- Carlson, T. N. and S. T. Arthur, 2000, "The Impact of Land Use—land Cover Changes Due to Urbanization on Surface Microclimate and Hydrology: a Satellite Perspective," *Global and Planetary Change*, 25:49–65.
- Driver, N. E. and B. M. Troutman, 1989, "Regression Models for Estimating Urban Storm-runoff Quality and Quantity in the United States," *Journal of Hydrology*, 109:221–236.
- Frazer, L., 2005, "Paving Paradise: The Peril of Impervious Surfaces," *Environmental Perspectives*, 113(7):A457–A462.
- Freund, R. J. and R. C. Littell, 2000, *SAS System for Regression* (third ed.), Cary, NC: SAS Institute.
- Galli, J., 1990, *Thermal Impacts Associated with Urbanization and Stormwater Best Management Practices*, Washington, DC: Department of Environmental Programs, Metropolitan Washington Council of Governments.
- Gallo, K. P., McNab, A. L., Karl, T. R., Brown, J. F., Hood, J. J., and J. D. Tarpley, 1993, "The Use of a Vegetation Index for Assessment of the Urban Heat Island Effect," *International Journal of Remote Sensing*, 14(11):2223–2230.
- Grossman-Clarke, S., Zehnder, J. A., Stefanov, W. L., Liu, Y. B., and M. A. Zoldak, 2005, "Urban Modifications in a Mesoscale Meteorological Model and the Effects on Near-Surface Variables in an Arid Metropolitan Region," *Journal of Applied Meteorology*, 44(9):1281–1297.
- Hall, M. J., 1984, *Urban Hydrology*, London, UK and New York, NY: Elsevier Applied Science Publishers.
- Heisler, G. M., Grant, R. H., Grimmond, S., and C. Souch, 1995, "Urban Forests—Cooling Our Communities?," in *Proceedings of the Seventh National Urban Forest Conference*, Kollin C. and M. Barretts (Eds.), Washington, DC: American Forests, 31–34.
- Horner, R. R., Booth, D. B., Azous, A. A., and C. W. May, 1997, "Watershed Determinants of Ecosystem Functioning," in *Effects of Watershed Development and Management on Aquatic Ecosystems: Engineering Foundation Conference, Proceedings, Snowbird, Utah, August 4–9, 1996*, Roesner, L.A. (Ed.), 251–274.
- Huang, Y. J., Akbari, H., Taha, H., and A. H. Rosenfeld, 1987, "The Potential of Vegetation in Reducing Summer Cooling Loads in Residential Buildings," *Journal of Climate and Applied Meteorology*, 26:1103–1116.
- Jenerette, G. D., Harlan, S. L., Brazel, A., Jones, N., Larsen, L., and W. Stefanov, 2007, "Regional Relationships between Surface Temperature, Vegetation, and

- Human Settlement in a Rapidly Urbanizing Ecosystem,” *Landscape Ecology*, 22:353–365.
- Jonsson, P., 2004, “Vegetation as an Urban Climate Control in the Subtropical City of Gaborone, Botswana,” *International Journal of Climatology*, 24:1307–1322.
- Klein, L. R., 1962, *An Introduction to Econometrics*, Englewood Cliffs, NJ: Prentice Hall, 1962.
- Lo, C. P. and D. A. Quattrochi, 2003, “Land-Use and Land-Cover Change, Urban Heat Island Phenomenon, and Health Implications, a Remote Sensing Approach,” *Photogrammetric Engineering and Remote Sensing*, 69(9):1053–1063.
- Lo, C. P., Quattrochi, D. A., and J. C. Luvall, 1997, “Application of High-Resolution Thermal Infrared Remote Sensing and GIS to Assess the Urban Heat Island Effect,” *International Journal of Remote Sensing*, 18(2):287–304.
- May, C. W., Horner, R. R., Karr, J. R., Mar, B. W., and E. B. Welch, 1997, “Effects of Urbanization on Small Streams in the Puget Sound Lowland Ecoregion,” *Watershed Protection Techniques*, 2(4):483–494.
- Myint, S. W. and N. S. N. Lam, 2005, “A Study of Lacunarity-Based Texture Analysis Approaches to Improve Urban Image Classification,” *Computers, Environment, and Urban Systems*, 29:501–523.
- Myint, S. W. and G. S. Okin, 2008, “Modeling Urban Land Covers Using Multiple Endmember Spectral Mixture Analysis,” *International Journal of Remote Sensing*, 30(9):2237–2257.
- Myrup, L. O., McGinn, C. E., and R. G. Flocchini, 1991, “An Analysis of Microclimate Variation in a Suburban Environment,” in *Seventh Conference of Applied Climatology*, Boston, MA: American Meteorological Society, 172–179.
- Oke, T. R., 1982, “The Energetic Basis of the Urban Heat Island,” *Quarterly Journal of the Royal Meteorological Society*, 108:1–24.
- Owen, T. W., Carlson, T. N., and R. R. Gillies, 1998, “An Assessment of Satellite Remotely Sensed Landcover Parameters in Quantitatively Describing the Climate Effect of Urbanization,” *International Journal of Remote Sensing*, 19:1663–1681.
- Pon, B., Stamper-Kurn, D. M., Smith, C. K., and H. Akbari, 1998, “Existing Climate Data Sources and Their Use in Heat Island Research” [<http://eetd.lbl.gov/EA/Reports/41973/>], last accessed October 24, 2008.
- Quattrochi, D. A., Luvall, J. C., Rickman, D. L., Estes, M. G., Jr., Laymon, C. A., and B. F. Howell, 2000, “A Decision Support Information System for Urban Landscape Management Using Thermal Infrared Data,” *Photogrammetric Engineering and Remote Sensing*, 66:1195–1207.
- Ridd, M., 1995, “Exploring a V-I-S (Vegetation–Impervious Surface–Soil) Model for Urban Ecosystem Analysis through Remote Sensing: Comparative Anatomy of Cities,” *International Journal of Remote Sensing*, 16:2165–2185.
- Roy, H. A., Rosemond, D. A., Paul, J. M., Leign, D. S., and B. J. Wallace, 2003, “Stream Macroinvertebrate Response to Catchment Urbanization (Georgia, USA),” *Freshwater Biology*, 48:329–346.
- Sailor, D. J., 1995, “Simulated Urban Climate Response to Modifications in Surface Albedo and Vegetative Cover,” *Journal of Applied Meteorology*, 34:1694–1704.
- Schueler, T., 1994, “The Importance of Imperviousness,” *Watershed Protection Techniques*, 1(3):100–111.

- Spronken-Smith, R. A. and T. R. Oke, 1998, "The Thermal Regime of Urban Parks in Two Cities with Different Summer Climates," *International Journal of Remote Sensing*, 19:2085–2104.
- Streutker, D. R., 2002, "A Remote Sensing Study of the Urban Heat Island of Houston, Texas," *International Journal of Remote Sensing*, 23:2595–2608.
- Taha, H., 1996, "Modeling Impacts of Increased Urban Vegetation on Ozone Air Quality in the South Coast Air Basin," *Atmospheric Environment*, 30:3423–3430.
- Upmanis, H., Eliasson, I., and S. Lindqvist, 1998, "The Influence of Green Areas on Nocturnal Temperatures in a High-Latitude City (Göteborg, Sweden)," *International Journal of Climatology*, 18:681–700.
- U.S. EPA, 1997, *Urbanization and Streams: Studies of Hydrologic Impacts*, Washington, DC: U.S. Environmental Protection Agency, Office of Water, EPA 841-R-97-009.
- Voogt, J. A. and T. R. Oke, 2003, "Thermal Remote Sensing of Urban Climates," *Remote Sensing of Environment*, 86:370–384.
- Wagrowski, D. M. and R. A. Hites, 1997, "Polycyclic Aromatic Hydrocarbon Accumulation in Urban, Suburban and Rural Vegetation," *Environmental Science and Technology*, 31(1):279–282.
- Weng, Q., 2001, "A Remote Sensing–GIS Evaluation of Urban Expansion and Its Impact on Surface Temperature in the Zhujiang Delta, China," *International Journal of Remote Sensing*, 22(10):1999–2014.
- Weng, Q., Lu, D., and J. Schubring, 2004, "Estimation of Land Surface Temperature–Vegetation Abundance Relationship for Urban Heat Island Studies," *Remote Sensing of Environment*, 89:467–483.
- Zhou, L., Dickinson, R. E., Tian, Y., Fang, J., Li, Q., Kaufmann, R. K., Tucker, C. J. and R. B. Myneni, 2004, "Evidence for a Significant Urbanization Effect on Climate in China," *Proceedings of the National Academy of Sciences, USA*, 101:9540–9544.